

Trigonometric Kriging: A New Method for Removing the Diurnal Variation From Geomagnetic Data

SERGE SEGURET

Centre de Géostatistique de Fontainebleau, Ecole des Mines de Paris

PHILIPPE HUCHON

Département de Géologie, Ecole Normale Supérieure, Paris

In order to remove the effect of the diurnal fluctuation of the magnetic field from magnetic measurements recorded at sea, we propose a new method: trigonometric kriging. This method is a particular case of the classical kriging method, but in this case we estimate locally a drift function of the form $D(t_i) = A_i \cos(\omega t_i) + B_i \sin(\omega t_i)$ or a truncated Fourier series, using a kriging neighborhood both in time and space. This method does not require any crossing point, which is a major advantage over previously published methods. After presenting the theoretical basis, we show how to put it into practice, i.e., how to choose, both in space and time, the set of points used for the estimation (kriging neighborhood) and how to determine experimentally the model for the generalized covariance which was used in the estimation. Trigonometric kriging has some interesting properties, such as to be exact at track crossings (if any), to allow an only "almost" periodic drift to be estimated, and finally to make possible filtering and gridding in one operation. Trigonometric kriging has been applied successfully to several sets of geomagnetic data recorded at sea near the equator, and we show two actual examples in Peru and in Indonesia.

INTRODUCTION

The geomagnetic field depends not only on internal causes but also on external effects such as the effect of solar wind on the layer *E* of the ionosphere, creating diurnal (or solar quiet day) variation due to the rotation of the Earth (24-hour period), and solar storms. This variation, called *Sq* (for Solar Quiet day) or *Sq(H)* variation also possesses an annual variation with its maximum in local summer, a semiannual variation with maxima near the equinoxes, a solar cycle variation related to the intensity of the solar flux [Hibberd, 1985]. Orbiting of the moon (28-day period) also creates variations due to the tidal forces acting on the ionosphere. Another minor source of variation, with a 27-day period, is due to the rotation of the Sun. Practically, only diurnal variations are to be removed from the geomagnetic anomalies, especially near the magnetic dip equator, where the variation is magnified and can reach 200 nT peak-to-peak [Smith, 1967]. Figure 1 shows the location of the magnetic dip equator and a plot of the horizontal component of the variation versus latitude. This plot clearly shows peak variations in excess of 200 nT in the equatorial region. Consequently, no analysis of magnetic data in equatorial regions should fail to consider the effects of diurnal variations [Handschumacher, 1976]. Moreover, oceanic magnetic anomalies are weaker near the equator, so that the *S/N* ratio (oceanic anomalies/diurnal variations) becomes very low and generally makes the data impossible to contour and difficult to interpret. One possible solution to this problem is to have a

reference station either at sea or on land, where the geomagnetic field is measured. However, this is not always possible, and, in the case of an on-land observatory, the station may be too far from the survey area, resulting in wrong estimates of the diurnal variations. An illustration is given in figure 2, where the top plot is the diurnal variation recorded at the Huancayo observatory (Peru). These data show a typical 24-hour periodic variation. Maximum values are -100 and +110 nT. However, variations in amplitude, shifts in frequency as well as higher frequency variations exist. The bottom plot shows the magnetic anomalies recorded during the same period during SEAPERF cruise off Peru [Pautot et al., 1986; Huchon and Bourgois, 1990], about 600 km away from the observatory. Maximum values range from -250 to 120 nT.

In this paper we propose a new method, trigonometric kriging (TK), to extract the diurnal variation from the recorded data, needing neither a reference station nor track crossings. For this reason, our method completely differs from the previous methods which all need information at cross tracks. In addition to simple methods such as the weighted linear interpolation proposed by Mittal [1984], which does not really consider the diurnal variation, there are two main approaches to estimate the diurnal variation. In the first set of papers a continuous function is computed in order to minimize cross-track differences using a least squares or regression analysis. Yarger et al. [1978] use a polynomial power series while Sander and Mrazek [1982] model the diurnal variation by a Fourier series. In the second approach proposed by Cloutier [1981] and developed by Cloutier [1983] and Ray [1985], a discrete, nonparametric solution is sought, which is then fitted to a continuous function. Once again, all these methods use only information at cross tracks, opposite to the method we propose.

Copyright 1990 by the American Geophysical Union.

Paper number 90JB01407.
0148-0227/90/90JB-01407\$05.00

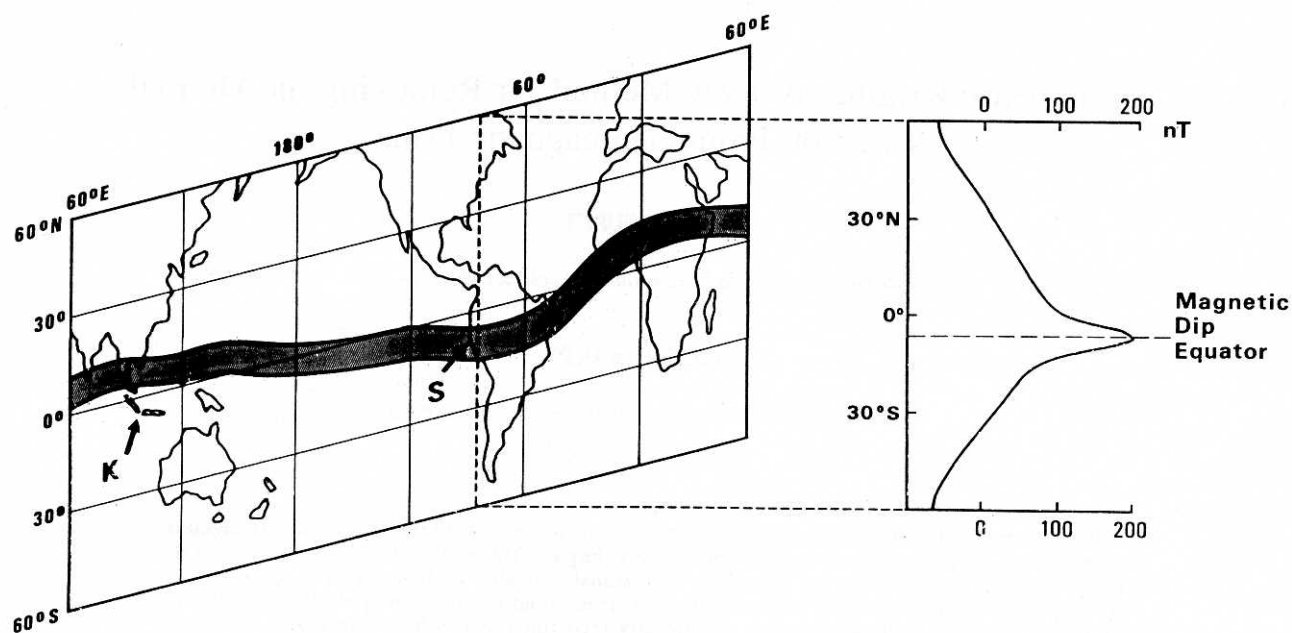


Fig. 1. (Left) Location of the magnetic dip equator. S, K are locations of the SEAPERC and KRAKATAU cruises, respectively. (Right) Peak-to-peak diurnal variation as a function of latitude at the longitude of Peru [from Handschumacher, 1976].

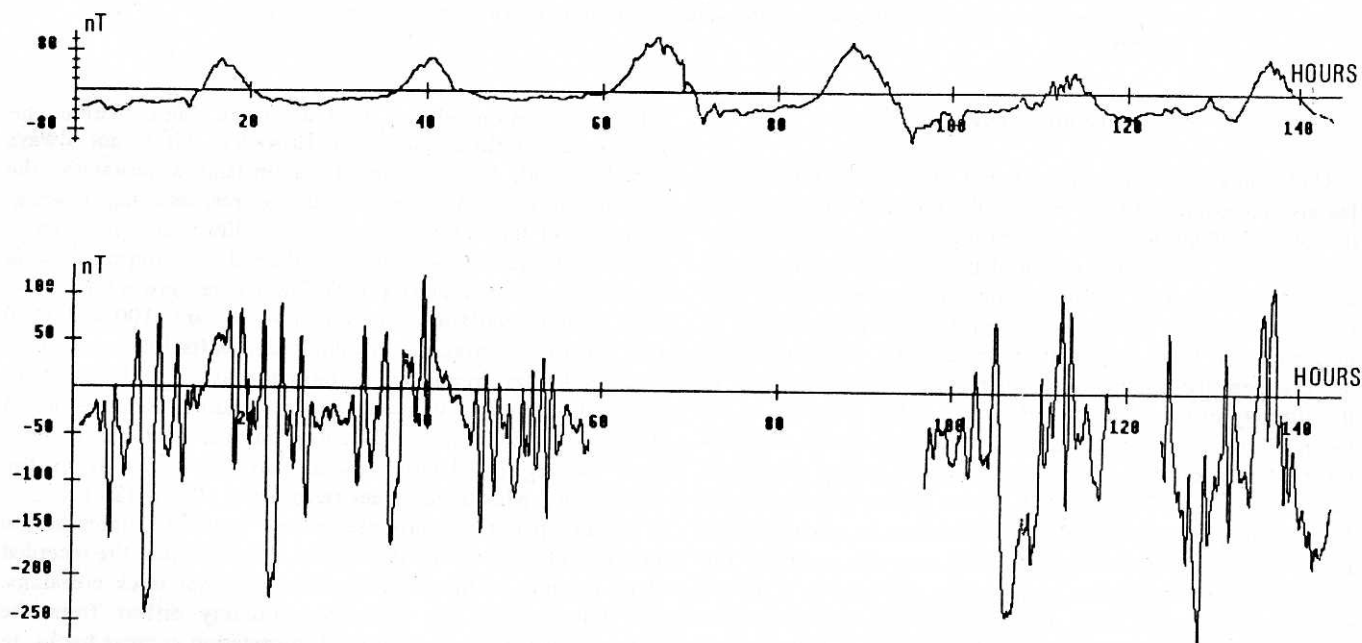


Fig. 2. (Top) Diurnal variation recorded at the Huancayo observatory (latitude $12^{\circ}5'S$, longitude $75^{\circ}10'W$, altitude 3300 m) from July 22 to July 28, 1986. Abscissa is time in hours starting at 0000 UT on July 22. (Bottom) Magnetic anomaly data recorded over the Mendana area during the SEAPERC cruise (see Figure 3) as a function of time.

We first present the theoretical background of TK and how to put it into practice. Then we discuss some interesting properties of TK and compare it to other methods. Trigonometric kriging has been successfully applied to magnetic data recorded during the SEAPERC and KRAKATAU cruises of the French R/V *Jean Charcot* in 1985 and 1986. These cruises were located off Peru and off Sunda Strait (Indonesia), near the equator. Due to the low values of the magnetic anomalies and to significant diurnal variations, the data were difficult to contour and to interpret before correction.

Since observatory data were available at the time of the cruises, we were able to check the results by comparison with the actual diurnal variation.

TRIGONOMETRIC KRIGING THEORY

Introduction

This new method is based on the theory of intrinsic random functions of order k (IRF- k) which was developed by Matheron

[1973] (see Appendix 1). Trigonometric kriging is a particular case of the more general kriging method and was first developed for a time signal [Séguret, 1987a] before being successfully extended to the space-time domain [Séguret, 1989]. At the outset, geostatistics was basically concerned with mining geology problems. However, it was gradually used to solve problems of modeling, estimation and simulation of natural phenomena in such varied fields as petroleum geology, pollution, meteorology, oceanography and more recently marine geophysics. Its formalism is based on identifying data to random functions (RF) [Matheron, 1965, 1971].

Objectives of the Trigonometric Kriging

Let $Z(\mathbf{x}, t)$ be the RF representing the magnetic anomaly recorded at sea, where \mathbf{x} is a vector of coordinates in space (latitude and longitude) and t is time. We want to split it up into a spatial and a time component:

$$Z(\mathbf{x}, t) = Y(\mathbf{x}) + D(t) \quad (1)$$

where $Y(\mathbf{x})$ is an IRF- k in space, independent of time and $D(t)$ the RF in time which represents the unknown diurnal variation.

The problem is thus to estimate a component of a global variable. It applies to the dichotomy (1) for geomagnetic data, but also to the decomposition (in space) into superficial and deep anomalies in gravimetry and magnetism [Chiles and Guillen, 1984]. Geostatistics offer a solution to the problem: factorial kriging analysis. Moreover, it has been shown theoretically that factorial kriging analysis can be a substitute to spectral analysis [Matheron, 1982], two methods which have been compared in practice [Galli, 1984; Chiles and Guillen, 1984]. The theoretical equivalence does not imply identical results, since the methodology differs. Any spectral analysis needs regularly spaced data and so depends on the preliminary gridding technique. Moreover, the spectral analysis proceeds globally on the scale of the complete measurement field, whereas kriging analysis, because of its moving neighborhood (see below), only requires the hypothesis of local stationarity in order to be operational.

The crucial problem is now to use an a priori model of the diurnal variation which is both based on the natural situation and is easy to handle mathematically. As $D(t)$ is only almost periodic in so far as its amplitude and its phase vary in time (and space at large scale), we set

$$D(t) = A \cos(\omega t) + B \sin(\omega t) \quad (2)$$

where A , B and ω are random but locally stationary at our scale of estimation (the so-called kriging neighborhood). To say that $Y(\mathbf{x})$ is an IRF- k does no harm in most cases in so far as the degree of regularity of the RF can be as high as we want (see Appendix 1).

Formalizing the Problem

Following the methodology given in classical geostatistics, we decide to estimate the function $D(t)$ at each measurement point $Z(\mathbf{x}, t)$ of the magnetic anomaly, using a linear estimator of the form:

$$D^*(t) = \sum_{\alpha} \lambda_{\alpha} Z(\mathbf{x}_{\alpha}, t_{\alpha}) \quad (3)$$

where $\{Z(\mathbf{x}_{\alpha}, t_{\alpha})\}$ is the set of measurement points which we want to use for the estimation. It constitutes the so-called kriging neighborhood, which is both a spatial and time neighborhood. In practice, when considering spatial estimations, it is customary to take points in the immediate spatial neighborhood of \mathbf{x} if the estimation is to be done of $Z(\mathbf{x})$. Later, we shall see that in our particular case we had to alter this practice in order to perform sampling in time also. In expression (3), the λ_{α} coefficients represent the unknowns of our problem.

As usual in geostatistics, the estimator $D^*(t)$ should satisfy the nonbias condition and minimize the variance of the error committed when we replace the (unknown) reality $D(t)$ by its estimator $D^*(t)$, that is to say,

$$E[D(t) - D^*(t)] = 0 \quad (4)$$

$$\text{Var}[D(t) - D^*(t)] \text{ min} \quad (5)$$

where the expressions $E[\]$ and $\text{Var}[\]$ represent the mathematical expectation and variance, respectively. The significance of the constraint (4) is that we wish to get a succession of estimations $D(t_i)$ which are lying on the same reference level. Expression (5) represents a quality criterium of the estimation, the notion of variance being a distance in the Hilbert space of the RF $D(t)$, a distance which it would be reasonable to minimize.

Setting Up the Equations

In what follows we shall pay particular attention to defining a certain number of constraints on the unknown coefficients λ_{α} in order to be able to express and minimize the variance of error (5) while respecting the non-bias condition (4). Combining expressions (1), (2) and (3), the error of estimation is written

$$\begin{aligned} D(t) - D^*(t) &= A \cos(\omega t) + B \sin(\omega t) \\ &\quad - \sum_{\alpha} [\lambda_{\alpha} (Y(\mathbf{x}_{\alpha}) + D(t_{\alpha}))] \\ &= A [\cos(\omega t) - \sum_{\alpha} \lambda_{\alpha} \cos(\omega t_{\alpha})] \\ &\quad + B [\sin(\omega t) - \sum_{\alpha} \lambda_{\alpha} \sin(\omega t_{\alpha}) - \sum_{\alpha} \lambda_{\alpha} Y(\mathbf{x}_{\alpha})] \quad (6) \end{aligned}$$

At this point, the hypothesis of local stationarity of A and B is used, since we assume that A and B are constant for the set $\{t\} \cup \{t_{\alpha}\}$. In order to eliminate time in expression (6), we impose

$$\sum_{\alpha} \lambda_{\alpha} \cos(\omega t_{\alpha}) = \cos(\omega t) \quad (7)$$

$$\sum_{\alpha} \lambda_{\alpha} \sin(\omega t_{\alpha}) = \sin(\omega t) \quad (8)$$

Then, the error of estimation (6) becomes

$$D(t) - D^*(t) = - \sum_{\alpha} \lambda_{\alpha} Y(\mathbf{x}_{\alpha}) \quad (9)$$

Practically, constraints (7) and (8) consist in fitting cosine and sine functions to the time trend of $Z(\mathbf{x}, t)$.

But these constraints (7) and (8) are not sufficient in order to obtain an expression of $\text{Var} [D(t) - D^*(t)]$. As a matter of fact, $Y(x)$ is an IRF- k and we also have to impose [Matheron, 1972a, 1973]

$$\sum_{\alpha} \lambda_{\alpha} f_L(x_{\alpha}) = 0 \quad \text{for each } L \leq k \quad (10)$$

where $f_L(x)$ are monomials of degree $L \leq k$ (note that L is a condensed notation: in one dimension, $f_L(x) = x^L$, but in two dimensions it is more complex as there are $(k+1)(k+2)/2$ monomials).

Let us call $K(h)$ the generalized covariance [Matheron, 1972b, 1973] (see Appendix 1) associated with $Y(x)$. If we enforce the set $\{\lambda_{\alpha}\}$ to verify (10), expression (9) becomes such as

$$E[-\sum_{\alpha} \lambda_{\alpha} Y(x_{\alpha})] = 0 \quad (11)$$

$$\text{Var}[-\sum_{\alpha} \lambda_{\alpha} Y(x_{\alpha})] = \sum_{\alpha} \lambda_{\alpha} \sum_{\beta} \lambda_{\beta} K_{\alpha\beta} \quad (12)$$

where $K_{\alpha\beta}$ is a short form of $K(h_{\alpha\beta})$, where $h_{\alpha\beta} = |x_{\alpha} - x_{\beta}|$ is the euclidian distance between points x_{α} and x_{β} . Expression (11) enables us to ensure the nonbias and (12) to obtain an expression of the variance of the error of estimation that we know how to minimize under the constraints (7), (8) and (10), by using Lagrange formalism. In this way, we obtain the following system

$$\sum_{\alpha} \lambda_{\alpha} K_{\alpha\beta} - \mu_1' \cos(\omega t_{\beta}) - \mu_2' \sin(\omega t_{\beta}) - \sum_L \mu_L f_L(x_{\beta}) = 0 \quad \text{for each } \beta \quad (13a)$$

$$\sum_{\alpha} \lambda_{\alpha} f_L(x_{\alpha}) = 0 \quad \text{for each } L \leq k \quad (13b)$$

$$\sum_{\alpha} \lambda_{\alpha} \cos(\omega t_{\alpha}) = \cos(\omega t) \quad (13c)$$

$$\sum_{\alpha} \lambda_{\alpha} \sin(\omega t_{\alpha}) = \sin(\omega t) \quad (13d)$$

Or in simplified matrix notation

$$\begin{bmatrix} K_{\alpha\beta} & f_L(x_{\alpha}) & \cos(\omega t_{\alpha}) & \sin(\omega t_{\alpha}) \\ f_L(x_{\beta}) & 0 & 0 & 0 \\ \cos(\omega t_{\beta}) & 0 & 0 & 0 \\ \sin(\omega t_{\beta}) & 0 & 0 & 0 \end{bmatrix} \begin{bmatrix} \lambda_{\alpha} \\ \mu_L \\ \mu_1' \\ \mu_2' \end{bmatrix} = \begin{bmatrix} 0 \\ 0 \\ \cos(\omega t) \\ \sin(\omega t) \end{bmatrix} \quad (14)$$

The λ_{α} coefficients represent the unknown solution of the system, and the μ_L coefficients the Lagrange multipliers. If P is

the number of points in the kriging neighborhood and k the degree of the IRF, $K_{\alpha\beta}$ is a $P \times P$ matrix, $f_L(x)$ a $P \times K$ matrix (with $K = k+1$ in one dimension and $K = (k+1)(k+2)/2$ in two dimensions), and $\cos(\omega t_{\alpha})$, $\sin(\omega t_{\alpha})$, $\cos(\omega t_{\beta})$, and $\sin(\omega t_{\beta})$ are P vectors. μ_1' , μ_2' , $\cos(\omega t)$, and $\sin(\omega t)$ are real values. Then the size of the matrix is $(P+K+2)^2$. See Appendix 1 concerning the conditions of regularity of this matrix.

PUTTING TRIGONOMETRIC KRIGING INTO PRACTICE

Putting this method into practice is facilitated by using the BLUEPACK software [Renard, 1986], in a configuration which is quite unusual, in so far as trigonometric functions are used as well as the customary polynomials. In this way, by using the methodology as defined by Matheron [1972a, b], determining the degree k of the IRF- k and the statistical inference of the generalized covariance $K(h)$ presents no problem. The only constraint is to impose the trigonometric functions as well as the usual monomials f_L , when recognizing the structure automatically.

Consequently, we are able to solve the TK system (14). The only remaining problem is that of choosing the set of measurements $\{Z(x_{\alpha}, t_{\alpha})\}$ which will be used for the estimation.

The Kriging Neighborhood: Global or Moving Neighborhood

The problem is to choose a set of measurements $\{Z(x_{\alpha}, t_{\alpha})\}$ on which we want to apply the TK system (14). In the first possible case (global neighborhood) we could decide to take all the measurements in the measurement field, whereas, in the second case (moving neighborhood) we shall only take some of them.

As in the case of a marine survey, we often have more than 10,000 points available in a measurement field, choosing a global neighborhood would imply having to invert a matrix of about 10,000 x 10,000 elements which is clearly excessive. We can add another argument in favor of the moving neighborhood. In fact, if the drift model (2) for the diurnal variation, where A and B are constant on a small space-time scale, is locally reasonable, it is, however, too restrictive globally, since this would require the daily drift $D(t)$ to be strictly periodic. However, these daily variations have an amplitude and frequency fluctuating in time at a fixed location (Figure 2) as well as depending on the space where the measurements are made. Choosing a moving neighborhood enables us to make local estimates of A and B or, in other words, a local estimation of the initial phase of the process. This series of local estimates gives us a global curve $D^*(t)$ which is not periodic in any way and is quite different from a trigonometric function.

Another advantage of the moving neighborhood is that we can make the approximation of a flat Earth when computing the distances, thus saving computing time. Such an approximation avoids using spherical coordinates, for which usual covariance functions are probably not relevant.

The Kriging Neighborhood: Sampling Taken in Time and Space

As TK is performed in space and time, when setting up the kriging neighborhood we cannot just take points which are in the same spatial neighborhood, but we must also consider

having a good sampling of points in time in order to carry out the estimation. That is why we shall oblige the neighborhood to contain sample points lying on several "data segments." A data segment is a portion of data a few hours long, practically between 3 and 12 hours depending on the configuration of the survey. Let us keep in mind that this constraint prevents the TK system (14) from only containing points coming from the same geophysical profile. Consequently, in practice the points in the kriging neighborhood lie on a few data segments so that it covers at least one period (24 hours) and are those which are the closest to the point to be estimated. But even there, we should be careful, for it may happen that two segments which are spatially close are distant in time by several days. In that case, mixing two sets of data containing different phases and amplitudes makes it difficult to adjust a single periodic trend. Let us remember that when setting up the TK equations we assumed the coefficients A and B to be locally stationary; here "locally" means both in space and in time. Consequently, it would be ideal to enforce the kriging neighborhood points used to estimate $D(t)$ to be also in a time interval of about 1 or 2 days around t .

Let us sum up by saying that putting TK into practice causes no problems as long as (1) we adopt a moving neighborhood; (2) the number of neighborhood points is sufficient to ensure good stability for the estimation (20 points are generally enough); (3) these points are taken in a spatial-time neighborhood which is near the location x we want to estimate and covers a period of 1 or 2 days around t .

Finding the Models

We briefly explain hereafter how we estimate the degree k of the IRF $Y(x)$ and its generalized covariance $K(h)$. See Renard [1988] for more details.

Estimating the degree k of the IRF. We divide the studied area into a large number of data subsets V_α containing the same number of points (as defined in this paper as the kriging neighborhood). We search for the degree k of the polynomials which, together with the trigonometric functions $\cos(\omega t)$ and $\sin(\omega t)$, fits optimally (in the least squares sense) the data contained in all subsets V_α . But filtering by least squares minimization is equivalent to kriging with a covariance reduced to the "nugget effect," i.e., corresponding to uncorrelated data, or white noise. Doing this with a large number of sets V_α enables us to elaborate statistics about the best order k in the studied area. This first step consists in identifying, at the scale of the kriging neighborhood V_α , the phenomenon (in space and time) as a sum of polynomials and trigonometric functions, i.e., to its trend. In the case of the estimation of the diurnal variation $D(t)$, we know the main frequency ω of the variation (24 hours), but we might generalize the method, the problem being to find the best couple (k, ω) that fits the data (in the least squares sense).

Evaluating the generalized covariance $K(h)$. The previous step gives us a couple (k, ω) which characterizes the space-time trend of the phenomenon. Now we choose, from a set of possible models for $K(h)$, the one that gives statistically the best results for all the selected sets V_α previously defined. Such models of $K(h)$ must fulfill certain conditions (see Appendix 1). Although the set of possible polynomial generalized covariances is infinite, in practice, the BLUEPACK software uses combinations of the four following functions: $a \delta_0(h)$ (nugget effect), $b h$ (linear), $c h^2 \ln(h)$ (spline) and $d h^3$

(cubic). The particularity of these models is that they depend linearly on coefficients (a, b, c, d) we can first compute, and second simply test by solving the kriging system for all the selected sets V_α , where we compare the data value to its estimation. Then we choose the model which gives statistically the best results. The practice shows, however, that the solution of the TK system is relatively insensitive to the model for $K(h)$.

The estimation of the degree k of the IRF and of the generalized covariance $K(h)$ are performed automatically in the BLUEPACK software. Finding k and $K(h)$ using 20,000 data points clustered in 1,000 sets V_α requires about 3 min CPU time on a VAX 11/780 computer.

TRIGONOMETRIC KRIGING PROPERTIES

Trigonometric Kriging Is Exact at Track Crossings

We now consider this question since most of the methods previously proposed in order to remove the diurnal variation use only this particular information provided by the misfits at track crossings. When the ship crosses back over its own route after several days, we have two measurement points $Z(x_1, t_1)$ and $Z(x_2, t_2)$ which are identical in space (i.e., $x_2 = x_1$), but distant in time of $dt = t_2 - t_1$, which gives a deviation dZ_{21} that is due theoretically to the diurnal variation:

$$dZ_{21} = Z(x_2, t_2) - Z(x_1, t_1) = D(t_2) - D(t_1) = dD_{21} \quad (15)$$

To show that TK is exact at track crossings is equivalent to demonstrate that

$$dD_{21} = D^*(t_2) - D^*(t_1) = dD^*_{21} \quad (16)$$

where $dD^*(t)$ is the estimation of $dD(t)$.

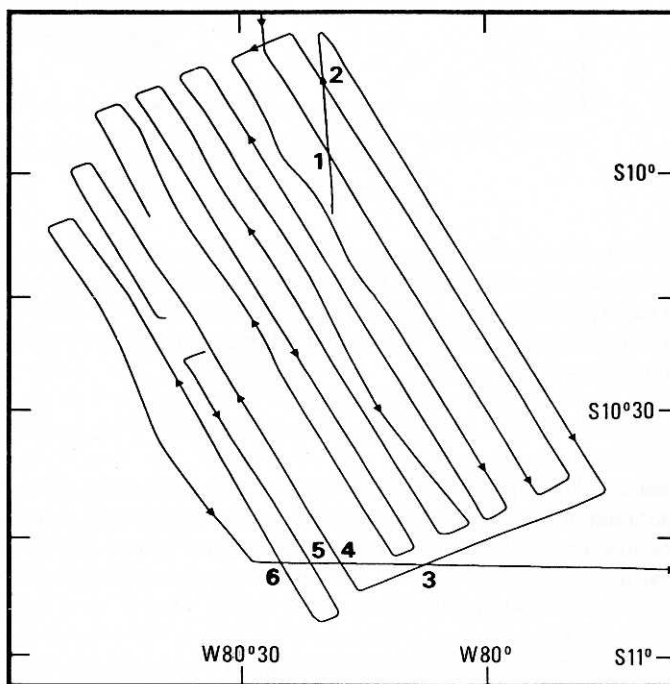


Fig. 3. Tracks chart over the Mendana area during the SEAPERC cruise. Numbers attached to track crossings refer to Table 1. Solid triangles delineate the data segments used in the kriging neighborhood search (see text).

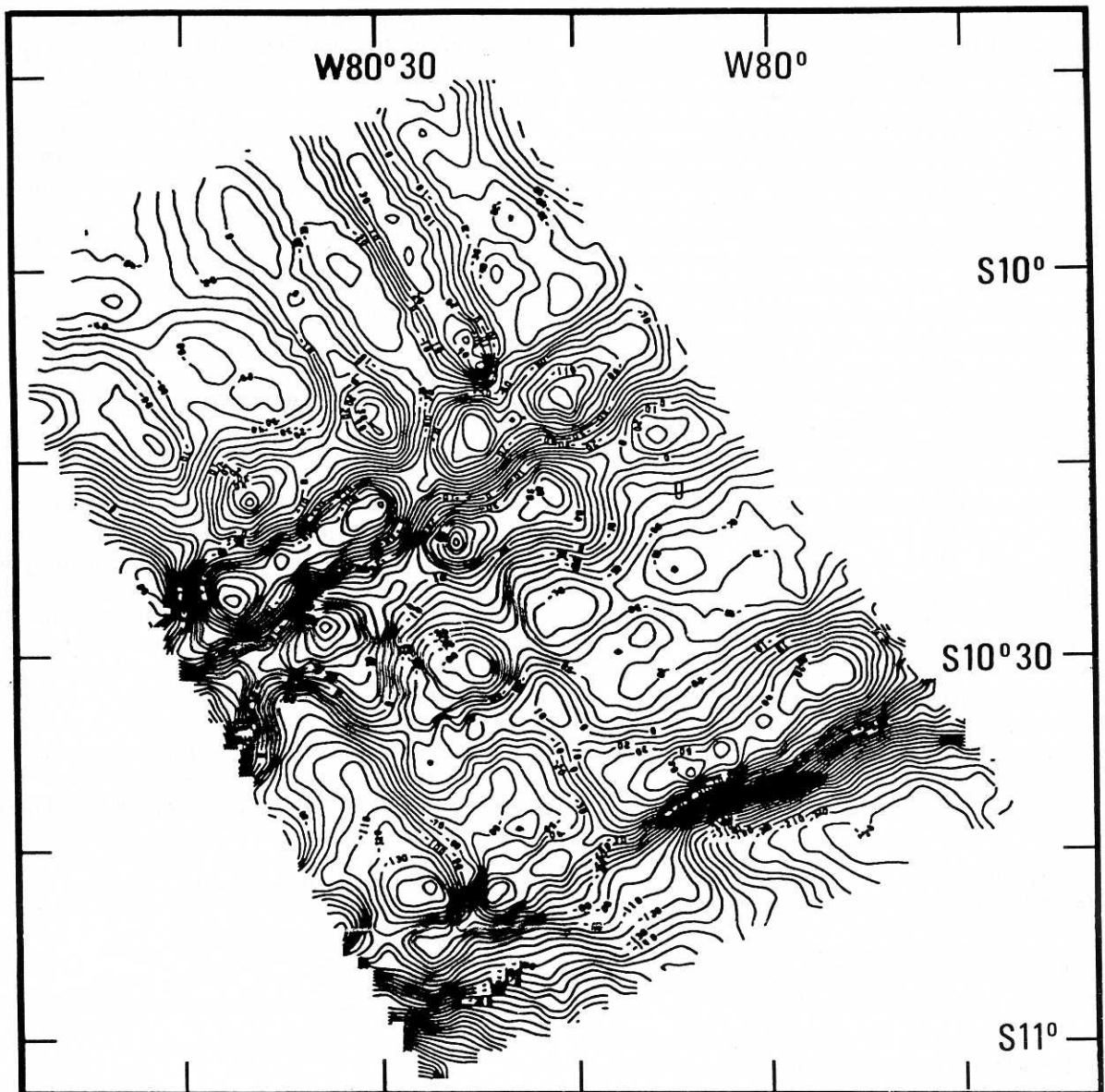


Fig. 4a. Contoured map of the magnetic anomaly data recorded over the Mendana area.

Suppose that the kriging neighborhood contains, among other points, a couple of track crossing points $Z(x_1, t_1)$ and $Z(x_2, t_2)$. Suppose that instead of evaluating $D(t_i)$, we want to estimate $Z(x_i, t_i)$ itself. Since we use linear estimators, we have the following property:

$$Z^*(x_i, t_i) = Y^*(x_i) + D^*(t_i) \quad (17)$$

where $Z^*(x_i, t_i)$, $Y^*(x_i)$ and $D^*(t_i)$ are estimators given by the solution of systems with the same matrix as system (14), but of course not the same right-hand side. Now since we use a kriging estimator, we also have a well-known property: kriging is exact on the data points; then

$$Z^*(x_i, t_i) = Z(x_i, t_i) \quad (18)$$

for each point (x_i, t_i) belonging to the kriging neighborhood. Since $x_1 = x_2$ and because of property (18), we have

$$dZ^*_{21} = Z^*(x_2, t_2) - Z^*(x_1, t_1) = D^*(t_2) - D^*(t_1) = dD^*_{21} \quad (19)$$

$$\begin{aligned} dZ^*_{21} &= Z^*(x_2, t_2) - Z^*(x_1, t_1) = Z(x_2, t_2) - Z(x_1, t_1) \\ &= Y(x_2) + D(t_2) - Y(x_1) - D(t_1) = D(t_2) - D(t_1) = dD_{21} \end{aligned} \quad (20)$$

Then by identifying (19) and (20), $dD_{21} = dD^*_{21}$, which means that TK is exact at track crossings.

In the same way, we could demonstrate that if two points $Z(x_1, t_1)$ and $Z(x_2, t_2)$ are not really identical, the score, as defined by

$$\text{Score} = dD^*_{21} - dD_{21} \quad (21)$$

has the expression

$$\text{Score} = \sum_j B^j (K_{j2} - K_{j1}) + \sum_L C_L (f_L(x_2) - f_L(x_1)) \quad (22)$$

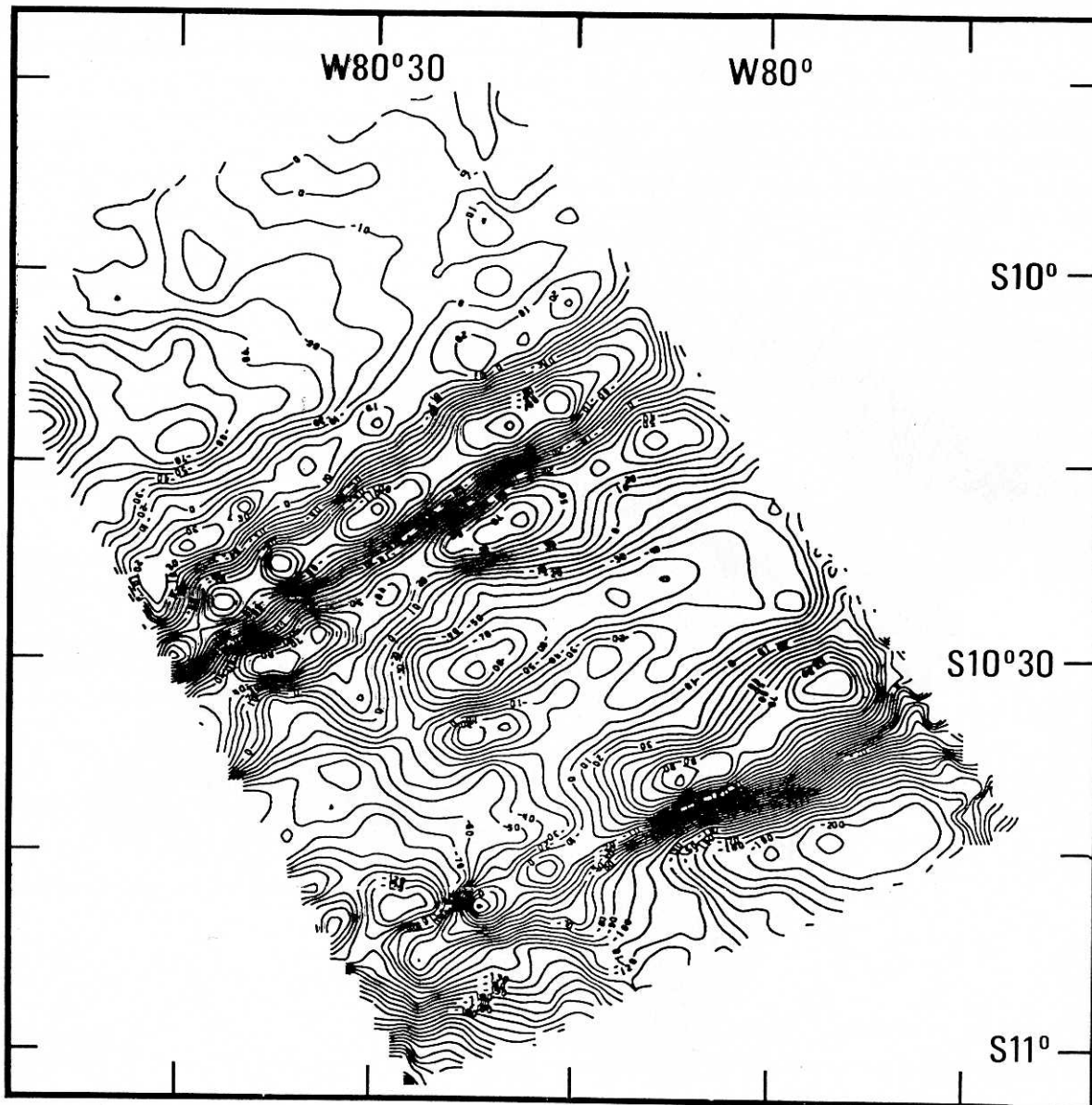


Fig. 4b. Contoured map of the magnetic anomaly data of Figure 4a corrected by removing the diurnal variation obtained from the Huancayo observatory (see Figure 2, top).

where B^j and C_L are components of the inverse matrix of TK system (14) multiplied by the data vector $Z(x_\alpha, t_\alpha)$, $K_{ji} = K(|x_j - x_i|)$ is the value of the generalized covariance along the distance between x_i and x_j , and f_L are the usual monomials. This expression (22) is proportional to the distance between the two points x_1 and x_2 .

To summarize, if the kriging neighborhood contains two points identical or nearly identical in space, the result of the estimation by TK will fit the cross-track difference.

This ability of TK to be constrained by cross-track differences can be a quality if the deviation at the crossing point dZ_{21} actually corresponds to the fluctuations $D(t)$. However, this is not always the case, as the following remarks show: (1) None of the crossing points are really the same and the distance between them, however small, corresponds to a difference in magnetic anomaly value which is not necessarily negligible, especially in areas with large gradient. Therefore looking for the identity between dD_{21} (difference due to the

diurnal variation) and dZ_{21} (observed difference at cross track) is nothing but a figment of the imagination. (2) Moreover, underway magnetic measurements are subject to errors of location. These can be significant. Consequently, two points which seem located almost at the same place can be quite far apart. This may cause a strong experimental deviation dZ_{21} which the diurnal variation $D(t)$ is unable to explain. Therefore the estimator $D^*(t)$ will take this deviation into consideration, whether it is real (due to $D(t)$) or fictitious (error of location), even if it means losing its time regularity. This phenomenon can be clearly seen on the estimated curve $D^*(t)$ in the case studies attached, where we see it literally "explode" toward extreme values before returning gently toward a periodic regularity. It might be thought that an estimator which is nonconditioned by the deviations at the crossing points (even if less precise) could be preferable, but any method involving the spatial and time structure of the phenomena under study will be dependent on these errors.

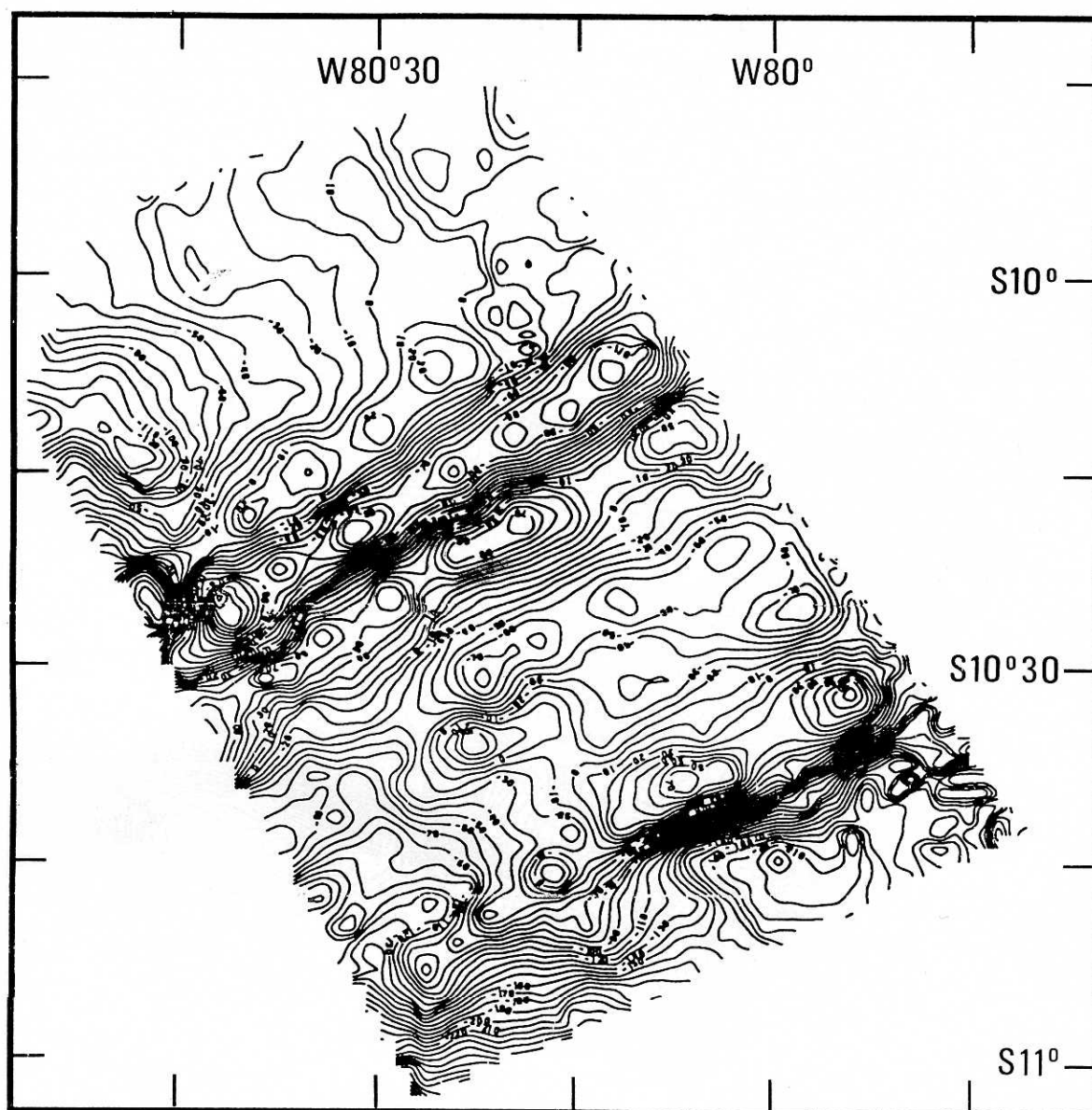


Fig. 4c. Contoured map of the magnetic anomaly data of Figure 4a corrected by removing the diurnal variation estimated by trigonometric kriging.

Consequently, for two points which are identical in space, the estimation will be conditioned by the cross-track difference which is due to the diurnal fluctuations. This TK property is interesting a priori since it makes it possible to follow the fluctuating phenomena $D(t)$ and to filter it. This was the objective we defined. Consequently, the study of scores as defined by relation (22) and applied in the two case studies attached is not a check on the theoretical properties of the estimator (since in theory the score is null), but rather an evaluation of the quality with which this method is put into practice. If we do not want the local estimation at cross points to be constrained by this property, we only have to impose that the kriging neighborhood does not contain such a couple of points.

TK Carries Out an Implicit Estimation of the Phase of the Initial Process $D(t)$

We could have envisaged creating an estimator (linear or not) based on periodic functions other than cosine and sine, since

the fluctuations $D(t)$ resemble a truncated trigonometric function more than a really sinusoidal curve (the amplitude of $D(t)$ is much smaller at night). We could have also thought of a roof-shaped function [Séguret, 1987b]. However, we have to use sine and cosine functions because it allows an implicit estimation of the phase of the initial process $D(t)$ since

$$A \cos(\omega t) + B \sin(\omega t) = C \cos(\omega t + \phi) \quad (23)$$

If, in practice, the initial phase ϕ does not constitute an insurmountable unknown (we know that $D(t)$ is generally maximum at 12:00 local time), the use of another type of periodic function which starts at this phase ϕ will assume that this model will follow its periodicity throughout the cruise. Now it has been seen that $D(t)$ is not strictly periodic. Therefore the moment will come when this model will be dephased in relation to reality. As we use a moving kriging neighborhood, the series of estimations contains implicitly an estimation of phase, and thus an implicit shift with respect to the initial phase of the fluctuations $D(t)$. It is precisely this

TABLE 1. Track Crossing Errors Over the Mendana Area

	t_1	t_2	dZ_{12}	dD^*	Er^*	dD^o	Er^o
1	22:12	21:12	-21.6	-16.0	-5.6	-20.9	-0.7
2	9:18	22:04	-21.0	-21.4	0.4	-32.3	11.3
3	7:50	16:01	4.0	4.7	-0.7	5.2	-1.2
4	9:05	15:05	4.8	5.9	-1.1	18.8	-14.0
5	2:40	14:45	29.0	29.3	-0.3	34.0	-5.0
6	4:27	14:25	-9.9	-8.7	-1.2	14.6	-24.5
Mean			15.1		1.5		9.4

Abbreviations are t_1 , local time on the first profile (hour:minute); t_2 , local time on the second profile; dZ_{12} , observed difference (in nT) in magnetic anomaly (2-1); dD^* , difference estimated by trigonometric kriging; Er^* , residual error ($dZ_{21}-dD^*$); dD^o , observed difference in observatory data; Er^o , residual error ($dZ_{21}-dD^o$)

property that enables us to estimate and filter a curve $D(t)$ which is only "almost" periodic.

This being said, if we want to improve the model by taking another type of periodic function, as each periodic function can be split into Fourier series and by truncating the series we get a good approximation with a minimum of frequencies, it is also possible to ask

$$D(t) = \sum_{i=1}^N A_i \cos(\omega_i t) + B_i \sin(\omega_i t) \quad (24)$$

and so to incorporate into the TK system $2N$ constraints of the type

$$\sum_{\alpha} \lambda_{\alpha} \cos(\omega_i t) = \cos(\omega_i t) \quad (25)$$

(and same in terms of sine). We then define the following system:

$$\begin{bmatrix} K_{\alpha\beta} & f_L(x_{\alpha}) & \cos(\omega_i t_{\alpha}) & \sin(\omega_i t_{\alpha}) \\ f_L(x_{\beta}) & 0 & 0 & 0 \\ \cos(\omega_i t_{\beta}) & 0 & 0 & 0 \\ \sin(\omega_i t_{\beta}) & 0 & 0 & 0 \end{bmatrix} \begin{bmatrix} \lambda_{\alpha} \\ \mu_L \\ \mu_1' \\ \mu_2' \end{bmatrix} = \begin{bmatrix} 0 \\ 0 \\ \cos(\omega_i t) \\ \sin(\omega_i t) \end{bmatrix} \quad (26)$$

The size of this matrix is $(P+K+2N)^2$ where P is the number of points in the kriging neighborhood, $K = (k+1)(k+2)/2$, k the degree of the IRF and N the number of frequencies. If the system (26) is correct in theory, its application may cause problems if we do not pay attention to the frequencies used in the truncated Fourier series (24). In fact, in system (26), if two frequencies ω_1 and ω_2 are too close together (e.g., 23 and 24 hours), although different, they can make the matrix of (26) singular, by the quasi identity of the two columns, this being dependent

on a choice of points in the kriging neighborhood which would be grouped in time.

Besides, we have set up trials and practice shows that a system matching a single frequency (if it is of 24 hours) is quite enough to solve the problem. Even better, the TK system (14) has been shown to be very stable in relation to the frequency used, i.e., it makes no difference if we take 23, 24 or 25 hours as our work frequency. The accuracy of this remark depends on a careful choice of the kriging neighborhood.

TK Makes Filtering and Gridding Possible in One Operation

Interpreting magnetic data often requires maps which necessitates the intermediate operation of gridding, enabling us to go from data on profile to data estimated at the nodes of a fixed sized grid. If we choose to use a linear estimator of type (3) for this gridding, it has been shown [Matheron, 1973] that kriging is the best possible estimator. Therefore besides the filtering of the time component $D(t)$, TK makes it possible to carry out the estimation of the spatial component $Y(x)$, where x is located at the node of a grid. For that the following system must be solved:

$$\begin{bmatrix} K_{\alpha\beta} & f_L(x_{\alpha}) & \cos(\omega t_{\alpha}) & \sin(\omega t_{\alpha}) \\ f_L(x_{\beta}) & 0 & 0 & 0 \\ \cos(\omega t_{\beta}) & 0 & 0 & 0 \\ \sin(\omega t_{\beta}) & 0 & 0 & 0 \end{bmatrix} \begin{bmatrix} \lambda_{\alpha} \\ \mu_L \\ \mu_1' \\ \mu_2' \end{bmatrix} = \begin{bmatrix} K_{\alpha x} \\ f_L(x) \\ 0 \\ 0 \end{bmatrix} \quad (27)$$

a system which makes it possible to estimate $Y(x)$ by an estimator $Y^*(x)$ of the form $Y^*(x) = \sum_{\alpha} \lambda_{\alpha} Z(x_{\alpha}, t_{\alpha})$. Here

we no longer estimate $D(t)$ at the measurement points (x_i, t_i) as in system (14), but $Y(x)$ at the nodes x of a grid. From now on, the system (27) ensures the gridding of $Y(x)$ and the filtering of $D(t)$. If this remark is obvious from a theoretical point of view, it is nonetheless methodologically important owing to the fact that the filtering is performed simultaneously with gridding, an operation which will be performed anyway.

TRIGONOMETRIC KRIGING COMPARED TO OTHER METHODS

Trigonometric Kriging Compared to Spectral Analysis

TK includes two methodological approaches: that of kriging analysis, as far as filtering is concerned and that of kriging in IRF- k (see Appendix 1). Indeed, the dichotomy (1) of the observed magnetic anomaly $Z(x, t)$ into two uncorrelated components $D(t)$ and $Y(x)$ is the departure point of the factorial kriging analysis.

Spectral analysis in space-time domain. Performing three-dimensional (3-D) Fourier transform in space and time would require a 3-D regular grid. Since measurements are made consecutively in time, we would have to extrapolate the data both in space and in time, which is clearly unreasonable.

Spectral analysis in time domain only. To solve the problem of filtering the diurnal variations by working in the time domain (i.e. considering $Z(x, t)$ as a function of time $Z(t)$ only) and filtering the 24-hour period (theoretical period of $D(t)$) by Fourier truncation, involves losing the spatial structural information in $Z(x, t)$. We applied this method on the data of the KRAKATAU 85 cruise [Séguret, 1987a]. The filtering was carried out perfectly, in fact too well carried out, as after the filtering by Fourier, the resulting signal was only white noise. The cause for this is that the KRAKATAU cruise was composed of 12-hour-long profiles which on the curve $Z(t)$ created an artificial 24-hour period comparable to that created by $D(t)$. So by filtering the 24-hour period, we also filtered the spatial signal which was made periodic by the ship's tracks. Only the spatial microstructures remain after filtering.

Consequently, filtering by Fourier transform in time is impossible if the profiles have a time-length close to 24, 12, 6 hours. Moreover, it would be a pity to study $Z(x, t)$ in time only and so lose all the spatial structural information.

Spectral analysis in space domain only (1-D). An alternative to Fourier transform in the time domain is to perform it in the space domain. This method can be used if the profiles are

reasonably linear, so that the measurements can be projected along the mean profile direction and then filtered profile by profile [Chamot-Rooke, 1988]. Note that such filtering, as is usual when using Fourier transform, requires us to interpolate the data in order to perform filtering on regularly spaced data. In practice, this method gives satisfactory results but requires careful checking of the part of the signal filtered out by this procedure. Also, the resulting track-crossing errors have no reason to be minimized by the procedure.

Spectral analysis in space domain only (2-D). Filtering the magnetic anomalies in the space domain using 2-D Fourier transform is inapplicable since it is impossible to detect a time periodicity in a regionalized signal in the space, unless we have data on a single profile, which is rarely the case. Moreover, it would then be easier to use 1-D Fourier filtering along the profile.

Comparison With Least Squares Minimization at Track Crossings

As the least squares techniques are not exact on the deviations at crossing points, this bias gives us a mean

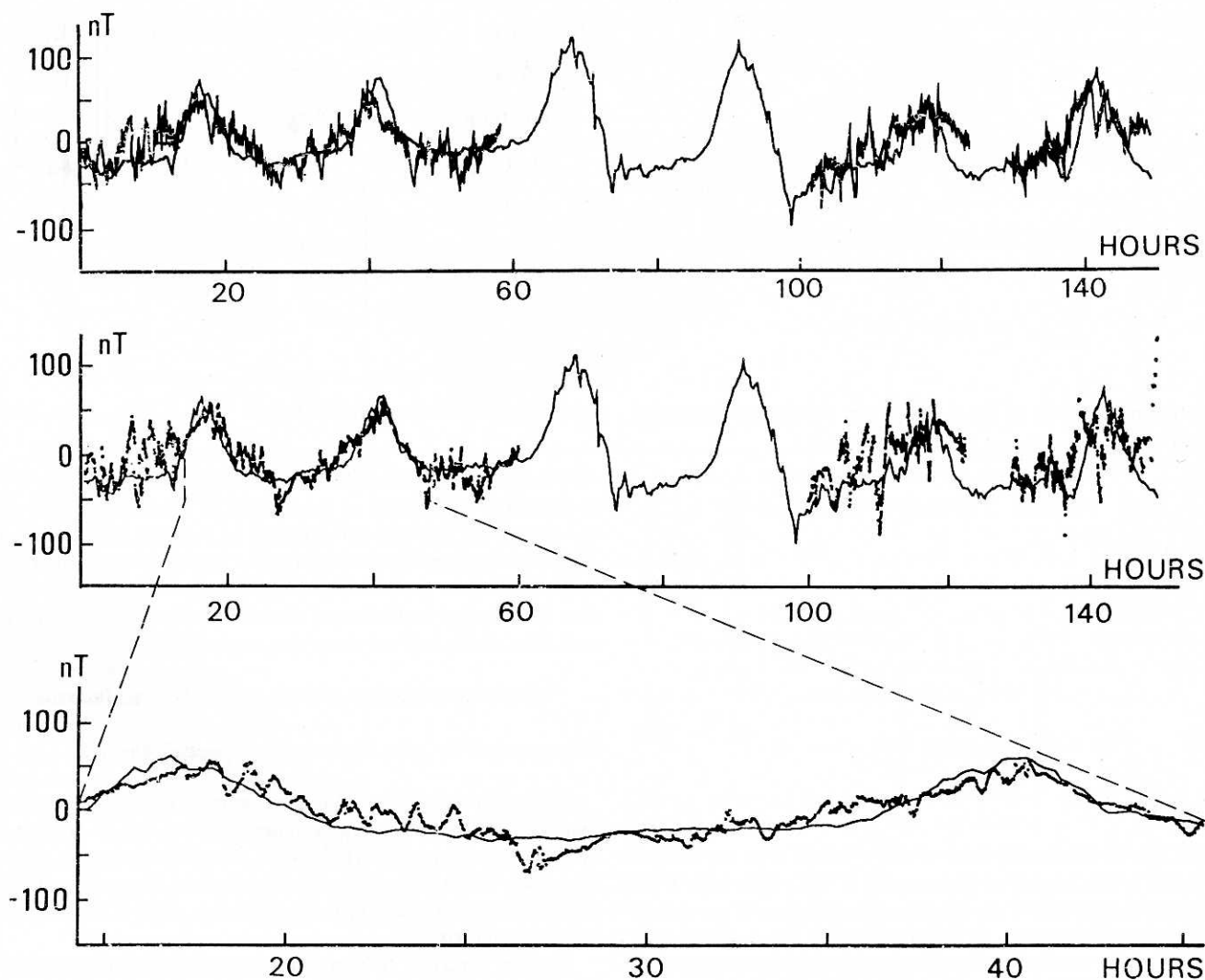


Fig. 5. Curves of the daily variation recorded at Huancayo observatory (solid curve) and estimated by trigonometric kriging (dotted curve). (Top) Using a kriging neighborhood of 20 points lying on 10 different data segments (see text). (Middle) Same but on seven different data segments. (Bottom) Enlargement of part of the middle curve.

estimation which is not very precise. This can be very efficient if we have lots of these points, which is not generally the case. If such points are numerous, least squares fit of polynomials [Yarger *et al.*, 1978] or of Fourier series [Sander and Mrazek, 1982] provides a good estimation of the diurnal variation curve. Using a different approach, Cloutier [1981, 1983] proposed a method which consists in the estimation of the unbiased, discrete function of minimum weighted variation which explains the observed differences at track crossings. Note that it is close to the constraints (4) and (5) we have used in TK. However, since the perturbation is estimated only at track crossings, it requires to fit a continuous function to the values in order to correct all the data. In other words, it is applicable if two conditions are satisfied: the number of track crossings should be large and the perturbation we are looking for should be as continuous as possible. This technique has been applied for reducing the radial ephemeris error present in Seasat geoid height data [Cloutier, 1981], where the conditions are obviously fulfilled. However, geomagnetic data recorded at sea generally do not meet these conditions. Moreover, it is obvious that if an inverse weighting scheme in time is used, this method would give the same result as obtained from trigonometric kriging by using track crossing points only.

APPLICATION OF TRIGONOMETRIC KRIGING TO ACTUAL DATA

Two sets of data were used to test TK: about 6,500 measured values (4 days) during the SEAPERC cruise over the Mendana area off Peru [Pautot *et al.*, 1986; Huchon and Bourgois, 1990] and 14,500 measured values (10 days) during the KRAKATAU cruise off Sunda Strait (V. Renard, personal communication, 1985). All measurements were collected at a rate of 1 per min. Analogous records of the geomagnetic field were obtained from the observatories of Huancayo (Peru) and Jakarta (Indonesia) and digitized at the same sampling rate of 1 min.

Seaperc Data Results

The magnetic data recorded along the track (Figure 3) are plotted as a function of time, as well as the diurnal variation curve recorded at the Huancayo observatory (Figure 2). Note that this observatory is located about 600 km away from the survey area. The corresponding contoured map (Figure 4a) displays an obvious track effect. Looking at the track chart (Figure 3) and at the data plotted as a function of time (Figure 2), we can see that the ship crossed periodically the same feature every 6 or 12 hours. An artificial periodicity is thus introduced into the data by the ship's track pattern. Only six crosspoints are available in the survey. The average of the absolute cross-track differences is 15.1 nT (Table 1).

The contoured map obtained using underway magnetic data corrected with the observatory data is shown in Figure 4b. The correction has removed almost all track effects. However, cross-track differences are still large with an average value of 9.4 nT (Table 1).

The curve estimated by trigonometric kriging follows quite well the curve recorded at the observatory (Figure 5). This shows that first the method gives pretty good results; second, the assumption of stationarity (in space) of the diurnal variations is valid (at this latitude) even at distances of several hundred kilometers.

In order to estimate the influence of the choice of the local

neighborhood in space (number of data points used) and in time (number and length of data segments used), we have performed two different estimations. The first one uses a neighborhood of 20 points on seven different, 6-hour-long data segments (corresponding to a kriging neighborhood in time of 1.75 days): the estimated curve shows anomalous spikes (Figure 5, center curve). The second one uses a neighborhood of 20 points on 10 different data segments (corresponding to a kriging neighborhood in time of 2.5 days): the spikes have disappeared and the estimated curve is smoother (Figure 5, top curve). We interpret this difference as due to the fact that when increasing the number of data segments, we better sample the signal in time, thus forcing it to be locally closer to the average period. This behavior occurs because we do not completely control the kriging neighborhood in time. In some cases, most of the points in the kriging neighborhood correspond nearly to the same local time: then, the signal is not correctly sampled in time and the estimates are inaccurate. In other cases where the points in the kriging neighborhood sample at least one period (24 hours) correctly, the estimate is less erratic and closer to the observatory curve. On the other hand, if the data are sampled on a few segments, the spatial neighborhood has a predominant influence on the estimate. However, we get a better score at track crossings using fewer segments. From a practical point of view, we thus have an easy way to adjust the estimated curve: the more segments we use, the smoother the curve we obtain. The less segments and the more points we use, the better we fit the track crossings.

Comparing the contour maps of the data corrected with the observatory curve (Figure 4b) and with the curve estimated by TK (Figure 4c), it appears that they are quite similar. The differences at track crossings using either the data corrected with the observatory data or the data filtered by TK are shown in Table 1. To be compared with the mean difference of 15.1 nT in the uncorrected data, applying the correction given by TK results in a mean 1.5 nT error. Recalling that in theory TK is exact at track crossings, it means that (1) the method has been correctly applied and (2) no serious navigation problems occurred.

Krakatau Data Results

This example of application is presented here in order to show how powerful TK is, even in difficult cases such as this cruise, in which the recorded magnetic anomalies range from 20 to 130 nT while the data from the Jakarta observatory range 75 nT peak-to-peak. The amplitude of the daily variation is thus of the order of magnitude of the recorded magnetic anomalies. Together with an average 12-hour length of the profiles in this systematic survey, it results in being impossible to interpret the magnetic anomaly, as shown by the contoured map of the measured values (Figure 6a). In fact this map shows a very strange pattern because cross-track differences are very large (often more than 50 nT). This map is to be compared with the map obtained after removing the daily variation by TK (Figure 6b), which obviously needs no comments.

CONCLUSIONS AND PERSPECTIVES

Trigonometric kriging has many theoretical advantages over methods for removing the daily variations proposed previously but above all TK has the main advantage of being applicable without cross points. This is probably the best argument in

favor of our method. Moreover, if cross points exist in the survey, the residual is theoretically null, and practically very small at these points.

However, trigonometric kriging has a shortcoming since the estimated curve $D^*(t)$ shows small amplitude and high-frequency variations about the average tendency. This results from the hypothesis of local stationarity of the coefficients A and B in the expression (2) of the drift model $D^*(t)$. Doing this, we do not impose any constraint on the regularity of the curve. Rather, we estimate a succession of values $D^*(t)$ where the coefficients A and B depend only on the kriging neighborhood, which we have said to be only partly controlled in time. Thus this method cannot be applied without carefully checking the kriging configuration around points where the estimate shows rapid fluctuations. Other problems when putting the method into practice include the geometrical configurations which make the TK system (14) singular, due to the use of polynomials of low degree. Fortunately, this seldom occurs.

Finally, we must point out that TK is applicable not only to magnetic data, but also to any kind of information which is regionalized (in space) and perturbed by an almost periodic drift

(in time or in space), such as measurements of temperature, pollution and activity of biota [Séguret, 1990].

APPENDIX 1: A FEW ELEMENTS OF IRF-K THEORY AND ITS APPLICATION

In order to make the reading of the paper easier for those not acquainted with geostatistics [Matheron, 1965, 1971], we present in this appendix (1) the theoretical basis for solving our problem, and (2) the conditions of regularity of the kriging system.

Aim of the Intrinsic Random Functions of Order k (IRF- k)

Formally, an IRF- k is a set of Random Functions (RF) $\{Z(x)\}$ which share two properties: (1) they have the same degree of regularity (degree k) and (2) they have the same generalized covariance $K(h)$.

More practically, it means that if we want to compute a weighted average of the particular RF $Z(x)$ using the relation

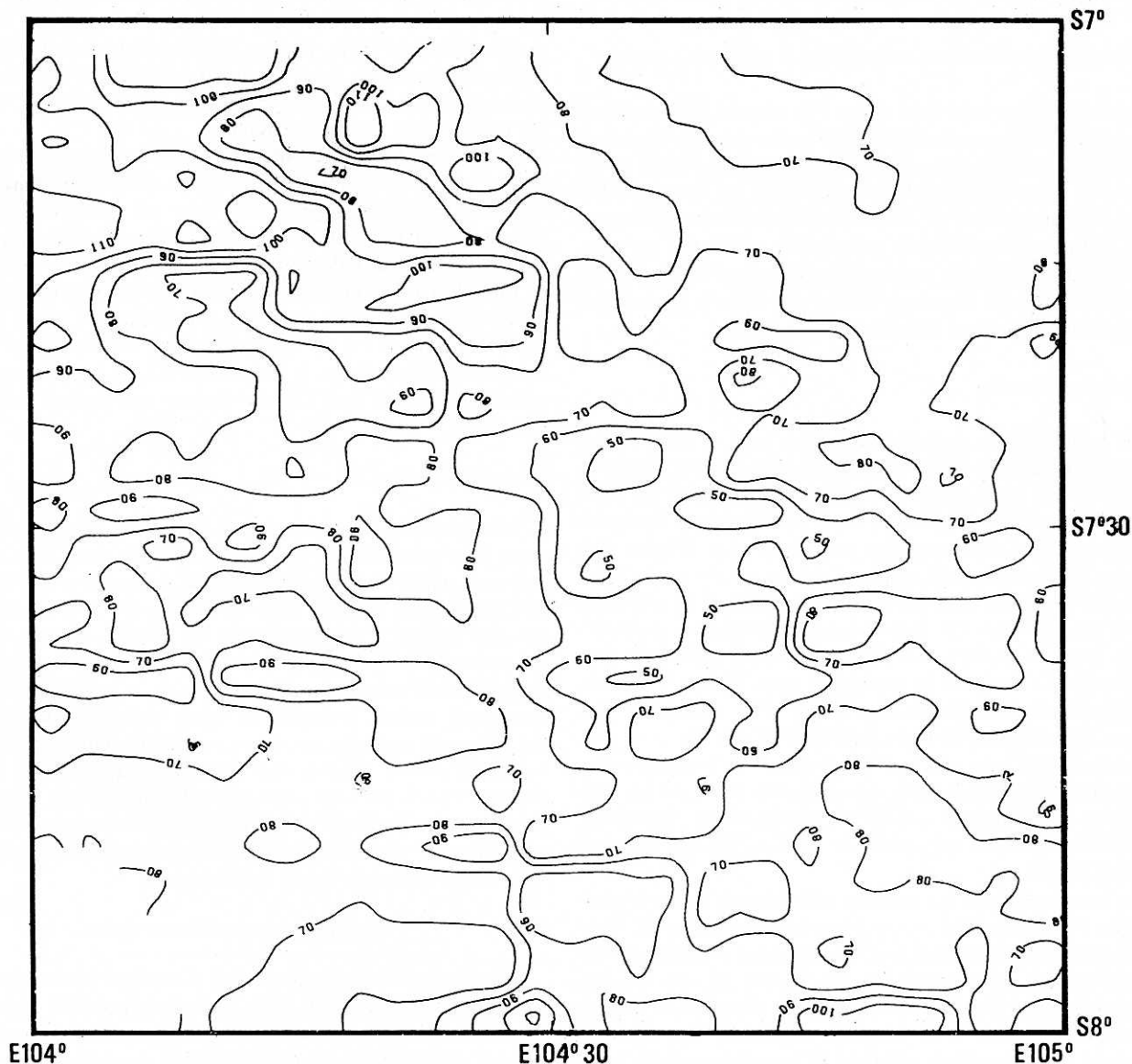


Fig. 6a. Contoured map of the magnetic anomaly data recorded during the KRAKATAU cruise.

$$Z^*(x) = \sum_{\alpha} \lambda_{\alpha} Z(x_{\alpha}) \quad (A1)$$

and if we want to obtain an expression of the variance of this average, we have to use particular sets $\{\lambda_{\alpha}\}$ because the expression (A1) does not have a variance for all $\{\lambda_{\alpha}\}$, except when $Z(x)$ is stationary. In this case, for any set $\{\lambda_{\alpha}\}$, the variance of the expression (A1) is

$$\text{Var} \left(\sum_{\alpha} \lambda_{\alpha} Z(x_{\alpha}) \right) = \sum_{\alpha} \lambda_{\alpha} \sum_{\beta} \lambda_{\beta} \text{Cov} (Z_{\alpha}, Z_{\beta}) \quad (A2)$$

where $\text{Cov} (Z_{\alpha}, Z_{\beta})$ is usually called the spatial covariance of $Z(x)$ (in the framework of the signal theory, this function is generally called autocovariance function). But stationary phenomena are not so usual.

When dealing with nonstationary phenomena, we solve this problem of obtaining an expression of the variance of (A1) by reducing the variability of the estimator $Z^*(x)$. For this, we

decide (in IRF- k theory) to use particular sets $\{\lambda_{\alpha}\}$ which filter out polynomials of degree k , i.e.,

$$\sum_{\alpha} \lambda_{\alpha} f_L(x_{\alpha}) = 0 \quad L = 0, 1, \dots, k \quad (\text{in one dimension}) \quad (A3)$$

where $f_L(x)$ are polynomials of degree k (k may be any positive integer, but in practice seldom greater than 2). Such a set $\{\lambda_{\alpha}\}$ which satisfies (A3) is called an "admissible linear combination of order k " (ALC- k) or admissible weights. We then expect that under these constraints (A3), the average (A1) has become a stationary random variable.

The second step is to define a function similar to the covariance in expression (A2) which, in this case, is called the generalized covariance $K(h)$. Matheron [1972b] has proved that such a function exists. Then if the set $\{\lambda_{\alpha}\}$ respects the constraints (A3), the variance of (A1) has the expression

$$\text{Var} \left[\sum_{\alpha} \lambda_{\alpha} Z(x_{\alpha}) \right] = \sum_{\alpha} \lambda_{\alpha} \sum_{\beta} \lambda_{\beta} K_{\alpha\beta} \quad (A4)$$

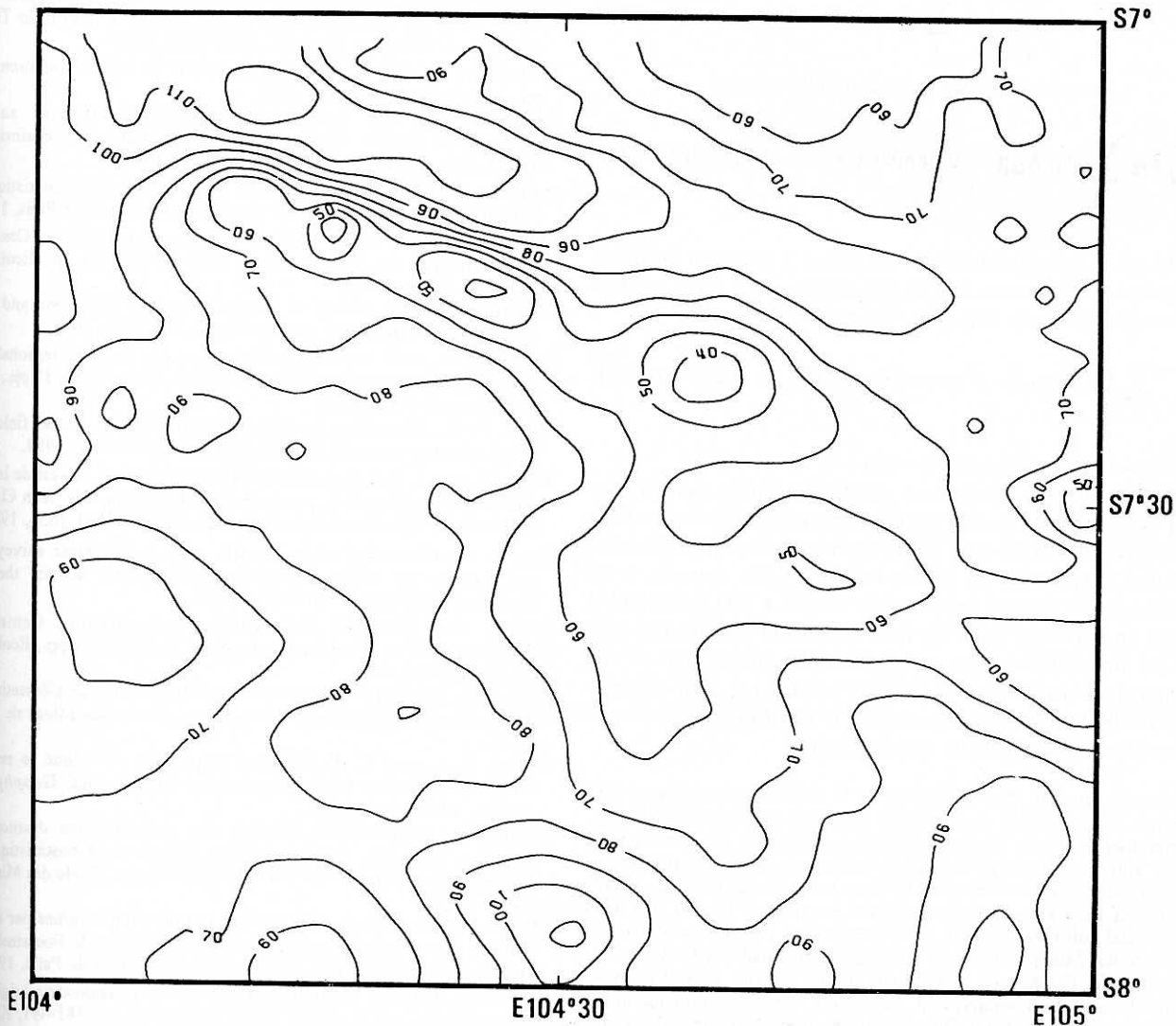


Fig. 6b. Contoured map of the magnetic anomaly data of Figure 6a, corrected by removing the daily variation estimated by trigonometric kriging.

where $K_{\alpha\beta}$ symbolizes $K(|\mathbf{x}_\alpha - \mathbf{x}_\beta|)$. Then the "kriging methodological algorithm" is possible, minimizing (A4) under the constraints (A3).

To summarize, we can say that the nonstationarity (in a large sense) of $Z(\mathbf{x})$ implies fitting most part of the phenomena by polynomials, so as to obtain residuals for which we can calculate and minimize the variance.

Regularity of the Kriging System

Systems (14), (26), and (27) share a common form:

$$[A](\lambda) = (b) \quad (A5)$$

where $[A]$ is a matrix and (λ) and (b) are vectors. This system must be invertible, so as to obtain the solution:

$$(\lambda) = [A]^{-1}(b) \quad (A6)$$

This is possible if the two following conditions are fulfilled:

(1) the generalized covariance $K(h)$ must be a strictly positive conditional definite function, which means that

$$\sum_{\alpha} \lambda_{\alpha} \sum_{\beta} \lambda_{\beta} K_{\alpha\beta} \geq 0 \quad (A7)$$

for each set $\{\lambda_{\alpha}\}$ of admissible weights

$$\sum_{\alpha} \lambda_{\alpha} \sum_{\beta} \lambda_{\beta} K_{\alpha\beta} = 0 \text{ implies } \{\lambda_{\alpha}\} = \{0, \dots, 0\} \quad (A8)$$

(2) the set $\{f_L(\mathbf{x}_{\alpha}), \cos(\omega t_{\alpha}), \sin(\omega t_{\alpha})\}$ must not be linear dependent, which means that if, for any $(\mathbf{x}_{\alpha}, t_{\alpha})$, there exists a vector of coefficients (C_L, C'_1, C'_2) so that

$$\sum_L C_L f_L(\mathbf{x}_{\alpha}) + C'_1 \cos(\omega t_{\alpha}) + C'_2 \sin(\omega t_{\alpha}) = 0 \quad (A9)$$

then $C_L = 0$ for each L and $C'_1 = C'_2 = 0$.

More practically, these two conditions imply that (1) we must use particular models for the generalized covariance $K(h)$ and (2) we must take care of the geometrical configuration of the data $\{Z(\mathbf{x}_{\alpha})\}$ we use for the estimation. For example, if we use data points located on a straight line in a 2-D space and if $Z(\mathbf{x})$ is an IRF-1 (of order 1), then systems (14), (26), and (27) will be singular. Another example: if the spatial part of the phenomenon is an IRF-0 and if data $\{Z(\mathbf{x}_{\alpha}, t_{\alpha})\}$ are sampled periodically in time with a frequency ω equal to that used in the system, the system will be also singular.

Acknowledgments. We warmly thank V. Renard, who initiated this research and provided us with data from the KRAKATAU cruise. Observatory data from Huancayo (Peru) were obtained by courtesy of L. Ocola. This work has been done partly under a contract with IFREMER. Computations were performed at the Centre de Géostatistique de l'Ecole des Mines de Paris, using a modified version of the BLUEPACK commercial software, initially developed and at present maintained at the Ecole des Mines. Comments and suggestions made by G. Matheron, X. Le Pichon, P. Chauvet, H. C. Nataf and D. Renard, as well as by A. Tarantola and two anonymous reviewers, greatly contributed to improving the manuscript. This is contribution 94 of the Laboratoire de Géologie de l'ENS.

REFERENCES

- Chamot-Rooke, N., Le bassin de Shikoku de sa formation à l'écaillage intraocéanique - Modèle tectonique et mécanique, *Mém. Univ. Pierre et Marie Curie, Paris*, 88-27, 295 pp., 1988.
- Chiles, J. P., and A. Guillen, Variogrammes et krigeages pour la gravimétrie et le magnétisme, in *Computers in Earth Sciences for Natural Resources Characterisation*, edited by J. J. Royer, pp. 455-468, Annales Ecole nat. sup. Géol. appl. prosp. min. du C.R.G. de Nancy, France, 1984.
- Cloutier, J. R., A new technique for correcting satellite ephemeris errors indirectly observed from radar altimetry, *NAVOCEANO Tech. Rep. TR-246*, U.S. Nav. Oceanogr. Off., Bay St. Louis, Miss., 1981.
- Cloutier, J. R., A technique for reducing low-frequency, time-dependent errors present in network-type surveys, *J. Geophys. Res.*, 88(B1), 659-663, 1983.
- Galli, A., Factorial kriging analysis: A substitute for spectral analysis of magnetic data, in *Geostatistics for Natural Resources Characterisation, Part 1*, pp. 543-557, D. Reidel, Hingham, Mass., 1984.
- Handschumacher, D. W., Post-Eocene plate tectonics of the Eastern Pacific, in *The Geophysics of the Pacific Ocean Basin and its Margin*, *Geophys. Monogr. Ser.*, vol. 19, edited by G. H. Sutton, M. Manghnani and R. Moberly, pp. 177-202, AGU, Washington, D. C., 1976.
- Hibberd, F. H., The geomagnetic Sq variation - Annual, semi-annual and solar cycle variations and ring current effects, *J. Atmos. Terr. Phys.*, 47, 341-352, 1985.
- Huchon, P., and J. Bourgois, Subduction induced fragmentation of the Nazca plate off Peru: Mendana Fracture Zone and Trujillo Trough revisited, *J. Geophys. Res.*, 95, 8419-8436, 1990.
- Matheron, G., Les Variables Régionalisées et Leur Estimation, 305 pp., Masson et Cie, Paris, 1965.
- Matheron, G., The theory of regionalized variables and its applications, *Cahiers du Centre de Géostatistique de Fontainebleau, Rep. 5*, 211 pp., Ecole des Mines de Paris, 1971.
- Matheron, G., Compléments sur les FAI-k, Centre de Géostatistique de Fontainebleau, *Note N-285*, 15 pp., Ecole des Mines de Paris, 1972a.
- Matheron, G., Les covariances généralisées polynomiales, Centre de Géostatistique de Fontainebleau, *Note N-299*, 23 pp., Ecole des Mines de Paris, 1972b.
- Matheron, G., The theory of intrinsic random functions and their applications, *Adv. Appl. Probability*, 5, 439-468, 1973.
- Matheron, G., Pour une analyse krigéante des données régionalisées, Centre de Géostatistique de Fontainebleau, *Note N-732*, 38 pp., Ecole des Mines de Paris, 1982.
- Mittal, P. K., Algorithm for error adjustment of potential field data along a survey network, *Geophysics*, 49(4), 467-469, 1984.
- Pautot, G., et al., Fragmentation de la plaque Nazca à l'Ouest de la fosse du Pérou: Résultats de la campagne SEAPERF du N.O. Jean Charcot, juillet 1986, *C.R. Acad. Sci. Paris, Ser. II*, 303, 1651-1656, 1986.
- Ray, R. D., Correction of systematic error in magnetic surveys: an application of ridge regression and sparse matrix theories, *Geophysics*, 50(11), 1721-1731, 1985.
- Renard, D., Bluepack 3-D general presentation, Centre de Géostatistique de Fontainebleau, *Note N-22/86*, 61 pp., Ecole des Mines de Paris, 1986.
- Renard, D., Automatic structure recognition, Centre de Géostatistique de Fontainebleau, *Note N-31/88*, 12 pp., Ecole des Mines de Paris, 1988.
- Sander, E. L., and C. P. Mrazek, Regression technique to remove temporal variation from geomagnetic survey data, *Geophysics*, 47(10), 1437-1445, 1982.
- Séguret, S., Magnétisme: Filtrage des perturbations diurnes par krigeage universel trigonométrique, Centre de Géostatistique de Fontainebleau, *Intern. rep. S-228/87/G*, 127 pp., Ecole des Mines de Paris, 1987a.
- Séguret, S., Magnétisme: Filtrage des perturbations diurnes par dérive externe trigonométrique, Centre de Géostatistique de Fontainebleau, *Intern. rep. S-229/87/M1*, 51 pp., Ecole des Mines de Paris, 1987b.
- Séguret, S., Filtering periodic noise by using trigonometric kriging, in *Geostatistics*, vol. 1, edited by M. Armstrong, pp. 481-491, Kluwer, Boston, Mass., 1989.

Séguret, S., Géostatistique du phénomène ondulatoire, Centre de Géostatistique de Fontainebleau, Ecole des Mines de Paris, in press, 1990.

Smith, E. K., Temperature-latitude sporadic *E*, in *Physics of Geomagnetic Phenomena*, edited by S. Matsushita and W. H. Campbell, pp. 615-623, Academic, San Diego, Calif., 1967.

Yarger, H. L., R. R. Robertson, and R. L. Wentland, Diurnal drift removal from aeromagnetic data using least-squares, *Geophysics*, **43**, 1148-1156, 1978.

P. Huchon, Laboratoire de Géologie & CNRS URA 1316, Ecole Normale Supérieure, 24 rue Lhomond 75231 Paris Cedex 05, France.

S. Séguret, Centre de Géostatistique de Fontainebleau, Ecole Nationale Supérieure des Mines de Paris, 35 rue Saint Honoré 77305 Fontainebleau Cedex, France.

(Received October 20, 1989;
revised March 23, 1990;
accepted June 18, 1990.)